Responses to the Comments of the Referees

Anonymous Referee #1

(1) The authors report on two experiments from a "new experimental method" that is really a combination of two existing methods: a thermodenuder and a dilution chamber. They use the model of Karnezi et al. (2014) to analyze the observations and extract volatility distributions for organic aerosol generated from meat charbroiling. The current study adds an explicit experimental element that was absent from the theoretical Karnezi et al. study. Given that the primary difference between this study and the Karnezi et al. study is the experimental measurement, I think that the manuscript requires much more detail regarding the experimental setup and what makes this new. Also, I think that the authors need to do a more complete job with data quality assurance, or at least need to convince me that their dilution measurements are correct. Finally, I think that the authors need to give more appropriate credit to work that has come before this. With substantial revision, I think that this paper could be acceptable for publication. Specific comments follow below.

We do appreciate the constructive comments and suggestions by the referee. We have done our best to address all of them and to improve the manuscript accordingly. Indeed, the present work is an effort to apply in the laboratory the approach suggested by the theoretical analysis of Karnezi et al. (2014). As expected, an experiment looks always a lot easier on paper (or as the output of a code) than in practice. The present work focuses on the experimental uncertainties (e.g., wall losses of particles) and also on some of the major assumptions (e.g., no losses of relatively volatile organic aerosol components and resulting evaporation in the line to the dilution chamber). More experimental details have been added together with an effort to better quantify the various uncertainties especially in the dilution measurements. We have also added material in the introduction to make sure that the appropriate credit is given to the publications that introduced the major ideas on which this work is based. These are described in more detail below in our responses to the specific comments of the referee.

(2) In their introduction, Louvaris et al. completely downplay the similarity of their work to the previous work of Grieshop et al. (2009, ES&T). The title if the Grieshop paper is "Constraining the Volatility Distribution and Gas-Particle Partitioning of Combustion Aerosols Using Isothermal Dilution and Thermodenuder Measurements." This is extremely similar to the title of the current paper: "Estimation of the volatility distribution of organic aerosol combining thermodenuder and isothermal dilution measurements." In the introduction, the authors mention that "Volatility measurements [by Grieshop] based on longer equilibration timescales were performed for POA from a diesel engine and wood combustion using isothermal dilution." But, they do not even mention that Grieshop also performed thermodenuder measurements. This seems to me like intentional obfuscation, especially since the authors also note that "Karnezi et al. (2014) proposed that volatility distribution of complex OA can be better constrained combining TD and isothermal dilution measurements," and later "we develop a new experimental technique to constrain the volatility distribution of organic aerosol using TD combined with isothermal dilution measurements following the suggestions of Karnezi et al. (2014)." Why mention Karnezi but not Grieshop in this context? Simply because one of the authors here is a co-author on the Karnezi paper but not the (earlier) Grieshop paper? I am concerned about this clear, seemingly intentional downplaying of previous measurements and methods.

We never intended to downplay the contributions of the Grieshop et al. (2009) work. Please note that several of the authors of the present papers are colleagues and close collaborators of the authors of the Grieshop et al. (2009) work. We have rewritten the paragraph describing the efforts to combine dilution and thermodenuder measurements making sure that the Grieshop et al. study receives the credit that it deserves for suggesting and applying the main idea on which the Karnezi et al. (2014) work was based resulting in the next step in the present work.

(3) The dilution experiments are insufficiently described. Was aerosol transferred once to the dilution chamber and then air sampled from it while the bag was allowed to collapse? Or was make up air continuously added? What was the flow rate through/out of the bag?
The aerosol was transferred once to the dilution chamber and its evolution with time was followed. No additional air was added in these experiments, so the dilution ratio was constant with time. The sampling flow rate from the dilution chamber was 1 L min^{-1}. This information has been added to the revised paper.

(4) Comparison of Fig. S3 and S4 indicates that for Experiment 2 the "corrected" number loss is 10-15% and, importantly, is very similar to the "corrected" mass loss. In other words, comparison between these figures suggests, at least to me, that the mass loss is entirely driven by number loss for this experiment. I have similar concerns regarding the dilution data for experiment 1, from comparison between Fig. S2 and Fig. S6. Put another way, it seems that the number-normalized mass loss for the dilution experiments is close to zero (MFR close to 1). To be convincing that the mass loss is real, I think that the authors need to consider the extent to which the particle size distribution shifted. Was shrinkage observed to an extent that is consistent with 10-15% mass loss? Currently, I do not find the "corrected" mass loss experimental observations convincing. Consequently, I have concerns over the resulting model interpretation of the observations and the entire paper.
This is a good point, as the dilution results are clearly sensitive to the accuracy of the wall loss corrections. We followed the suggestion of the reviewer and examined the aerosol number distributions to confirm that the particles were evaporating in the dilution chamber. In Experiment 1, the number mode diameter decreased from 93 nm to 87 nm corresponding to an 18% volume reduction. This is consistent with the 20% loss estimated after the wall loss correction. The shifting of the number distributions to smaller sizes was also obvious in the dilution data of Experiment 2. The corresponding change of the mode diameter was from 115 to 105 nm or a 24% reduction in volume. This information about the changes in the measured size distributions has been added to the manuscript to support the conclusions based on the loss-corrected measurements.

One important additional point can be made examining the estimated volatility distributions in Fig. 7. Based on the calculated uncertainty the mass fraction of the more volatile components (with C^* higher or equal to 10 μg m^{-3}) could be as low as zero. This corresponds to practically no evaporation during dilution. As a result, our estimates considering their uncertainties are quite robust. On the contrary, the dilution data help constrain the upper limit of the contributions of the more volatile components to the COA.

(5) L109: Since the authors are looking at "fresh" OA, it is unclear why OH radical concentrations are mentioned. D9 butanol is simply used as a dilution tracer.
We have deleted this discussion of the calculation of OH concentrations that is probably confusing for most of the readers. There was a second chemical aging stage in the main smog chamber experiment, but this is not relevant for the present work that focuses on fresh OA.

(6) L206 and Fig. 5: The experiments took nearly 8 h (30 mins at each of 15 temperatures). I think that the authors need to provide more information regarding exactly when the various

spectra were measured. Is the “ambient” spectrum an average over those 8 h? Is it the average of the two measurements that came before/after the 200 C measurement? How similar in time was the ambient spectrum to the 200 C spectrum? Related, how similar were the ambient spectra measured at the beginning of the measurement versus 8 h later at the end of the measurement? Have things evolved over time due to the particles being suspended in the chamber? Granted, the spectra are quite similar, as the authors note, but more detail is required. Further, the authors simply note that the spectra are similar. But, their calculations suggest that, perhaps, they should be different because the particle composition at ambient vs. 200 C is different. This should be discussed.
The spectrum of the ambient COA was practically constant during the experiment. The average spectrum is used in the paper. The theta angles between the spectra measured during the experiment and their average were all less than 2 degrees. The same stability characterized the spectra at 200 C. The angles between the individual measurements and the average spectrum were also less than 2 degrees. As a result, the comparison shown in Figure 5 is quite robust and applies throughout Experiment 1. This information about the stability of the measured mass spectra has been added to the revised manuscript.

The above results suggest that even if the cooking aerosol remaining at 200 C had quite different volatility than the ambient COA, the differences of their AMS spectra were modest. This is probably due to the fact that the AMS measures mainly the fragments of the corresponding organic molecules which probably had a lot of similarities in this case. A brief discussion of this point has been added to the paper.

(7) L217: The authors note that there are “small” differences between the two experiments. But I would argue that the differences, especially in the TD experiments, are actually quite large. I have included the figures from the paper below so that they can be directly compared. It is clear that the behavior at lower temperatures is dramatically different. One experiment indicates almost no evaporation until T > 80 C while the other indicates substantial (20% loss) evaporation at temperatures just over ambient. Further discussion is required.
We agree with the referee that the use of the term “small differences” is probably confusing. We focus on the actual differences of the evaporated fraction at different temperatures and avoid qualifying them as small or large. Please note that some differences are expected given that these are two different cooking experiments with different meat, potential small differences in cooking details, etc.

(8) L307 and elsewhere: The authors report the “average” volatility in a number of locations. First, it is not clear how this is calculated. Is it a linear average? A logarithmic average? Second, in reporting this number the authors seem to be making an a priori assumption that this is a meaningful number. This is not a value that is commonly reported. What is this mean meant to represent and how is it useful? I could have two very different distributions, for example one bimodal and one monomodal, that have the same average. These would exhibit very different behavior though.
This is a logarithmic average, something that is now explained in the paper. We think that it is a useful metric of changes of a volatility distribution when the same volatility range (volatility bins) are used. We agree that in other cases it may not be as helpful on its own, but here it expresses the change in the results due to the inclusion of the dilution measurements and we would prefer to keep it. In other cases, it could be accompanied by the standard deviation of the distribution to make it more useful.

Anonymous Referee #2

(1) This paper provided a new technique to measure/estimate the volatility distribution of organic aerosols by combining a thermodenuder (TD) and a dilution system. Cooking OA was used as an example to show the performance of this technique. In general, it could be a better technique than a separated TD system, which would be suffered by the possible processes occurred during the heating, e.g. thermal decomposition. The manuscript is overall well written and the topic fits the scope of AMT. I therefore recommend this manuscript can be published after some revision.
We appreciate the positive assessment of our work by the referee. Detail responses to the comments can be found below.

(2) More discussions/statements are needed to explain how these two systems are combined. What is the role of dilution system in estimating the volatility distribution of targeted aerosol?
The dilution data, at least in these experiments, help constrain the contributions of the more volatile organic aerosol components. These are the components with C^* higher or equal to 10 μg m^{-3} in this case (see Fig. 7). However, the dilution measurements cannot help constrain better the contributions of the LVOCs and ELVOCs to the organic aerosol composition. Even if the dilution results do not depend on the enthalpy of evaporation, their combination with the thermodenuder data does reduce the uncertainty of the corresponding estimate. These are now discussed in a new paragraph in the Conclusions section.

(3) How to understand the differences between the modelled and experimented data during isothermal dilution (Fig. 4b)? It looks that the evaporation only occurred during the first few minutes, but not a continuous evaporation. Will this influence the understanding and estimation of the volatility distribution?
This behaviour is quite useful in the estimation of both the volatility distribution of the cooking OA and the existence of any potential resistances to mass transfer. The prompt evaporation is interpreted by our model as evidence that any resistances to mass transfer in this system were modest. The resulting accommodation coefficients (evaporation coefficients in this case) were 0.06 and 0.07. The fact that only 20% of the COA evaporated during these first few minutes, suggests that the contribution of the more volatile OA components (IVOCs and part of the SVOCs) as also modest. After this 20% evaporated the system reached equilibrium and evaporation stopped. These useful insights from the behaviour of the dilution curve have been added to the paper.

(4) It is highly possible that COA contain some ELVOC, e.g. HULIS (Nie et al., 2017@ACP). I suggest the author to provide a more bin of ELVOCs?
This is a good point that deserves a little more attention. Almost all thermodenuder measurements stop at a temperature at which the MFR is not zero. In our case at 250 C, the MFR was approximately 5%. At least this fraction could in principle be ELVOCs. Our model adds this fraction to the lowest volatility bin used ($C^*=10^{-3}$ μg m^{-3}). In general, the contribution that appears in the lowest volatility bin refers to material that has volatility less or equal to the corresponding value. This point is now made in the paper together with a reference to the work of Nie et al. (2017) discussing the contributions of HULIS to ELVOCs.

(5) How to change the dilution time, by changing flow?
There are a number of ways to increase the time available for dilution measurements. One is to take less frequent samples from the dilution chamber. Use of lower flowrates can also work. One could also use larger dilution chambers, which also help achieve higher dilution

ratios, but are a lot more difficult to operate in the field. Please note however that in these experiments the COA reached equilibrium after 30 min, so the remaining 2 hours of dilution data helped only in confirming the equilibrium state of the system.

(6) Why the mass spectrums look so similar before and after heating or dilution (25 C vs 200 C)? The volatility of organics should be correlated to their oxidation state (e.g. O/C), molecular weight et al. (E)LOVC tends to have a higher oxidation state and large molecular weight. This indicates there should be some differences for the mass fragmentation between evaporated mass and remained mass. PMF could be used for the AMS measurements in case of several heating steps, to make the change of mass spectrums clearer, e.g. Hong et al., 2017@ACP.
The modest difference in the AMS spectra of all the COA and its less volatile components is indeed interesting. This is probably due to the fact that the AMS measures mainly the fragments of the corresponding organic molecules which probably had a lot of similarities in this case. If the differences in volatility of compounds coming from the same source were mainly related to differences in the size of the organic molecules and not so much to their chemical nature (acids, hydrocarbons, etc.) one would expect such behaviour. Please note that there are differences (a theta angle of 11 degrees does support this) but that at least from the point of view of the AMS these differences are modest. PMF does not help in this case, because for two factors it results in more or less the ambient and the 200 C spectra that have already been analysed. A brief discussion of this point has been added to the paper.

(7) Any ideas about the phase state of produced COA, which could influence the volatility measurement.
These experiments do not provide much information about the phase state of the produced COA. The relatively fast evaporation during dilution does suggest relatively small delays to evaporation consistent with an evaporation coefficient of 0.06-0.07. These have already been considered in the analysis. In the sensitivity analysis section (Section 3.2.1) we discuss the sensitivity of our results to these uncertain mass transfer resistances considering the case of evaporation coefficients of 0.01 and 0.1. These tests suggested that the enthalpy of vaporization is rather insensitive to the evaporation coefficient in this range, and that the SVOCs and LVOCs changed by less than 15%. These are discussed in the Sensitivity Analysis section.

(8) The residence time is effective residence time or total residence time? There would be a temperature profile in the thermodenuder? An effective residence time should be carefully considered.
The residence time of 14 s mentioned in the paper is the centerline residence time at 298 K. The temperature profile (both in the longitudinal and radial directions) in our TD has been analysed by Lee et al. (2010) and Gkatzelis et al. (2016). The change in volumetric flowrate due to the change in temperature along the TD is taken into account by the Riipinen et al. (2010) TD model used in this work. This information has been added to the manuscript.

(9) The given vaporization enthalpy of COA in this study is a universal value, or can only be used in this work?
The vaporization enthalpy of COA estimated here is applicable to pork meat char broiling. We do expect that it is a useful estimate for char broiling of other meat, but clearly this needs to be supported by other experiments. Its applicability to other types of cooking (e.g., frying) is unknown. We have added a qualifying statement about the use of the corresponding value.

Estimation of the volatility distribution of organic aerosol combining thermodenuder and isothermal dilution measurements

Evangelos E. Louvaris [1,2], Eleni Karnezi [3], Evangelia Kostenidou [2], Christos Kaltsonoudis [2,3], and Spyros N. Pandis [1,2,3]

[1] Department of Chemical Engineering, University of Patras, Patras, Greece

[2] Institute of Chemical Engineering Sciences, FORTH/ ICEHT, Patras, Greece

[3] Department of Chemical Engineering, Carnegie Mellon University, Pittsburgh, USA

Correspondence to: Spyros N. Pandis (spyros@andrew.cmu.edu)

Abstract

A method is developed following the work of Grieshop et al. (2009) for the determination of the organic aerosol (OA) volatility distribution combining thermodenuder and isothermal dilution measurements. The approach was tested in experiments that were conducted in a smog chamber using organic aerosol (OA) produced during meat charbroiling. A thermodenuder (TD) was operated at temperatures ranging from 25 to 250°C with a 14 s centerline residence time coupled to a High-Resolution Time-of-Flight Aerosol Mass Spectrometer (HR-ToF-AMS) and a Scanning Mobility Particle Sizer (SMPS). In parallel, a dilution chamber filled with clean air was used to dilute isothermally the aerosol of the larger chamber by approximately a factor of 10. The OA mass fraction remaining was measured as a function of temperature in the TD and as a function of time in the isothermal dilution chamber. These two sets of measurements were used together to estimate the volatility distribution of the OA and its effective vaporization enthalpy and accommodation coefficient. In the isothermal dilution experiments approximately 20% of the OA evaporated within 15 min. Almost all the OA evaporated in the TD at approximately 200°C. The resulting volatility distributions suggested that around 60-75% of the cooking OA (COA) at concentrations around 500 μg m^{-3} consisted of low volatility organic compounds (LVOCs), 20-30% of semi-volatile organic compounds (SVOCs) and around 10% of intermediate volatility organic compounds (IVOCs). The estimated effective vaporization enthalpy of COA was 100 ± 20 kJ mol^{-1} and the effective accommodation coefficient was 0.06-0.07. Addition of the dilution measurements to the TD data results in a lower uncertainty of the estimated vaporization enthalpy as well as the SVOC content of the OA.

1. Introduction

Atmospheric aerosols have a significant impact both on human health (Pope et al., 2009; Caiazzo et al., 2013) and on Earth's climate due to their ability to scatter and absorb solar radiation and their effects on cloud properties and lifetimes (IPCC, 2014). These particles consist of a wide variety of chemical compounds, with organic components representing 20-90% of their submicron mass (Zhang et al., 2007). Organic aerosol (OA) can be emitted directly as primary particles (POA) from various anthropogenic and natural sources or can be formed when gas-phase oxidation products of volatile (VOCs), intermediate volatility (IVOCs) and semi-volatile (SVOCs) organic compounds condense onto pre-existing particles forming secondary organic aerosol (SOA). There is limited knowledge of the sources, chemical evolution, and physical properties of OA due to the complexity of the mostly unknown thousands of constituents of OA. These uncertainties often lead to erroneous predictions of OA concentrations by chemical transport models.

Volatility is one of the most important physical properties of OA as it determines the partitioning of its components between the gas and particulate phases, and eventually their atmospheric fate (Donahue et al., 2012). One of the most common techniques to constrain indirectly aerosol volatility requires the use of a thermodenuder (TD). The aerosol enters a heated tube where the most volatile components evaporate leaving behind the less volatile species in the particulate phase (Burtscher et al., 2001; Kalberer et al., 2004; Wehner et al., 2002, 2004; An et al., 2007). TDs usually consist of two sections: the heating section where the aerosol evaporation takes place and the denuder/cooling section. This second section often contains activated carbon in order to prevent re-condensation of the evaporated components. The typical result of a TD is the mass fraction remaining (MFR) of the aerosol as function of the TD temperature. The MFR depends on aerosol concentration, size, vaporization enthalpy, and potential mass transfer resistances (Riipinen et al., 2010).

TD measurements of OA volatility have received considerable attention recently, and have been performed both in the field (Huffman et al., 2009; Cappa and Jimenez, 2010; Lee et al., 2010; Louvaris et al., 2017) and in the laboratory (Saleh et al., 2008; Faulhaber et al., 2009; Lee et al., 2011). Riipinen et al. (2010) argued that OA practically never reaches equilibrium in a TD at ambient concentration levels. TD measurements were performed by Lee et al. (2010, 2011) using multiple residence times. These authors argued that use of multiple residence times in the heating section of the TD can help to decouple mass transfer effects from thermodynamics. Similar conclusions were reached also by Riipinen et al.

(2010) and Cappa (2010). Saleh et al. (2012) used a particle concentrator upstream of a TD in order to achieve higher ambient aerosol loadings so that the system could reach equilibrium. Their results suggested accommodation coefficient values around 0.3 for the ambient aerosol that they examined. Volatility measurements based on longer equilibration timescales were performed for POA from a diesel engine and wood combustion using isothermal dilution (Grieshop et al., 2009). Cappa and Wilson (2011) studied the evolution of the OA mass spectra from lubricating oil and a-pinene oxidation as the particles were heated. They concluded that there were high mass transfer resistances for the SOA produced from α-pinene ozonolysis. Saleh et al. (2013) measured the equilibration timescales for the gas to particle partitioning of SOA formed from α-pinene ozonolysis using an accommodation coefficient of the order of 0.1.

Grieshop et al. (2009) suggested that combination of thermodenuder and dilution measurements can better constrain the OA volatility over a wide range. Karnezi et al. (2014) proposed an algorithm for the combination of the two types of measurements and the derivation of the optimum ~~that~~ volatility distribution of ~~complex~~ OA and its uncertainty.~~can be better constrained combining TD and isothermal dilution measurements.~~ Kolesar et al. (2015) combining rapid isothermal dilution with TD measurements argued that the volatility of SOA formed from α-pinene ozonolysis is mostly independent of the SOA loading during temperature-induced evaporation.

Most of the previous studies discussed above determined the OA volatility assuming a-priori values for the OA vaporization enthalpy and accommodation coefficient. Since the TD results are sensitive to these values large uncertainties were reported for the volatility distributions. The performance of different time scale measurements can, in principle at least, allow the estimation of the volatility distribution together with the vaporization enthalpy and accommodation coefficient with lower uncertainty ranges.

In this study, we continue the development of the ~~develop a new~~ experimental technique of Grieshop et al. (2009) to constrain the volatility distribution of organic aerosol using TD combined with isothermal dilution measurements using~~following~~ the algorithm~~suggestions~~ of Karnezi et al. (2014). The OA mass fraction remaining is measured as a function of temperature in the thermodenuder and as a function of time in a dilution chamber in parallel. TD measurements are corrected for size- and temperature- dependent losses and the dilution system measurements for size-dependent losses. These two sets of measurements are then used together with the approach of Karnezi et al. (2014) to estimate the volatility distribution of the OA and its effective enthalpy of vaporization (ΔH_{vap}) and effective accommodation coefficient (a_m). Cooking OA is used as an example for the application of the method.

2. Experimental description

Smog chamber experiments were conducted in the FORTH smog chamber to constrain the volatility distribution of fresh OA emissions from meat charbroiling. The experimental setup is shown in Fig. 1. A metal bellows pump (model MB 602, Senior Aerospace) was used to transfer cooking emissions to the 10 m^3 Teflon chamber. Details for the meat charbroiling and the transferring process can be found in Kaltsonoudis et al. (2016a). A TD (Louvaris et al., 2017) was placed upstream of a High-Resolution Time-of-Flight Aerosol Mass Spectrometer (HR-ToF-AMS Aerodyne Research Inc.) (Decarlo et al., 2006; Canagaratna et al., 2007) measuring the size-composition of the submicron non-refractory material, and a Scanning Mobility Particle Sizer (SMPS 3936 TSI) measuring the particle size distribution. A dilution Teflon chamber (1 m^3) was used for the isothermal dilution. The VOCs and the dilution ratio (DR) were measured by a PTR-MS (Ionicon Analytic). ~~The OH radical concentrations were estimated using I~~isotopically labeled butanol (1-butanol-d9, Sigma) was added to the chamber to assist in the measurement of the dilution ratio. ~~The change of the concentration of the PTR-MS *m/z 66* was used to calculate the OH concentrations based on the second-order reaction of d9-butanol with the OH radicals. The corresponding reaction constant used is 3.4 x 10^{-12} cm^3 $molecule^{-1}$ s^{-1} (Barmet et al., 2012).~~

The SMPS was operated at a sampling flow rate of 1 L min^{-1} and sheath flow rate of 5 L min^{-1} sampling every 3 minutes. The HR-ToF-AMS was sampling every three minutes with 0.1 L min^{-1} and was operated in the higher sensitivity mode (V-mode) (DeCarlo et al., 2006). The PTR-MS was sampling with 0.5 L min^{-1}. Details about the PTR-MS operation can be found in Kaltsonoudis et al. (2016b).

The TD was operated at temperatures ranging from 25 to 250°C using 15 temperature steps for about half an hour per step. Sampling from the main chamber was alternated between bypass and TD every 3 min with computer-controlled valves. The changes in the particle mass concentration and size were measured by both the HR-ToF-AMS and the SMPS resulting in thermograms of the MFR as a function of the TD temperature. The OA MFR was calculated as the ratio of organic mass concentration of a sample passing through the TD at time t_i over the average mass concentration of the ambient samples that passed through the bypass line at times t_{i-1} and t_{i+1}. The sample residence time in the centerline of the TD was 14 s at 298 K corresponding to an average residence time in the TD of 28 s. The temperature profile in our TD (both in the longitudinal and radial directions) has been analysed by Lee et al. (2010). The change in volumetric flowrate due to the change in temperature along the TD is taken into account by the Riipinen et al. (2010) TD model used in this work.

The dilution chamber was initially partially filled with clean air. Then, the metal bellows pump was used to transfer cooking emissions from the main chamber to it, diluting them in the process to close to ambient concentration levels. The aerosol was transferred from the main to the dilution chamber only once and then its evolution with time was followed. Dilution measurements were performed every 9 min by both the SMPS and the HR-ToF-AMS. The SMPS sampling flow rate was 1 L min^{-1}. The dilution ratio was calculated as the ratio of the PTR-MS *m/z 66* concentration of the main chamber over the PTR-MS *m/z 66* concentration of the dilution chamber. The dilution ratios during the isothermal dilution experiments are shown in Table 1 and were 10 ± 0.5 and 14 ± 0.5 for Experiments 1 and 2 respectively. These remained constant during the experiments. Table 1 also summarizes the characteristics of each experiment. The residence time in the dilution chamber was a few hours. The mass fraction as a function of time during isothermal dilution was measured as the ratio of mass concentration at time t_i over the initial mass concentration in the dilution chamber at time t_0.

2.1 Loss corrections

The thermodenuded OA was corrected for particle losses in the TD. Particle losses were measured as a function of the TD temperature and particle size using sodium chloride particles and the same flow rate as that used in the experiments. The average loss fraction in the 0.1-1 μm size range for each temperature was used for the correction of the AMS results and the accuracy of the correction was tested using the SMPS number distributions and the approach of Lee et al. (2010).

The OA concentrations during the isothermal dilution experiments were also corrected for size dependent wall losses during the experiments. These losses were calculated for each experiment using the number concentration distributions measured by the SMPS. Following Pathak et al. (2007) the wall loss rate constant $k_w(D_p)$ was estimated from least-square fits of the natural logarithm of the SMPS particle number distributions values for each size as a function of time in the latter stages of the experiment when evaporation was negligible. Fig. S1 shows these loss rate constants as function of particle size for Experiment 1. These size-dependent loss corrections were applied to the measured number distribution at each time step allowing the estimation of the corrected number and volume distributions. The accuracy of the corrections can be evaluated using the temporal evolution of the corrected total number concentration in the chamber. Given the low number concentrations (around 5000 particles cm^{-3}) coagulation is negligible and the corrected total number concentration should be approximately constant. The corrected number concentration varied by less than 10% during the three hours of the experiment (Fig. S2a). Even if the measured mass concentration was reduced by approximately 50% in the dilution chamber, the evaporation resulted in only 20% mass reduction (Fig. S2b). The other 30% was due to losses of particles to the walls of the dilution chamber. The change in the aerosol size distribution is consistent with the above result. In Exp. 1 the number mode diameter decreased from 93 nm to 87 nm corresponding to an 18% reduction in volume.

Similar results were obtained also during Experiment 2. The corrected number concentration varied by less than 5% (Fig. S3a), suggesting that the correction was quite accurate. The evaporation resulted in a 20% mass reduction as shown in Fig. S3b. The shifting of aerosol size distributions to smaller sizes was once more obvious. The aerosol number mode diameter decreased from 115 to 105 nm suggesting a 24% reduction in volume.

As another quality assurance test the mass fraction values measured by the SMPS were compared to those measured by the HR-ToF-AMS assuming that the collection efficiency of the latter remained constant as the OA evaporated (Fig. S4). The corresponding differences between the two measurements were a few percent or less.

2.2 Determination of the volatility distributions

The dynamic mass transfer model of Riipinen et al. (2010) together with the error minimization approach proposed by Karnezi et al. (2014) were used for the determination of the volatility distributions. Inputs for the model included the initial OA mass concentrations for the TD and the isothermal dilution chamber obtained by the HR-ToF-AMS, the initial particle sizes obtained by the SMPS, the residence times of both systems, and the dilution ratio of the isothermal dilution system. The initial mass concentration for the TD experiments was of the order of 10^2 μg m^{-3}. Table 1 summarizes these inputs of the model. The corrected mass fraction values determined by the HR-ToF- AMS were used as system inputs for the calculations.

The volatility distribution in the volatility basis set framework is expressed with a range of logarithmically spaced C^* bins along a volatility axis (Donahue et al., 2006). For our analysis a set of six volatility bins ranging from 10^{-3} to 10^{3} µg m^{-3} were used.

3. Results and discussion

3.1 Volatility distribution of cooking organic aerosol (COA)

Applying the approach of Karnezi et al. (2014) the volatility distribution of the COA was estimated. The distribution for Experiment 1 is depicted in Fig. 2. The average volatility, defined as the average $\log_{10}C^*$ weighted by the mass fraction of each bin was approximately 0.1 µg m^{-3}. This average volatility is a useful metric for the comparison of volatility distributions when the same volatility range is used. According to these results the COA at around 550 µg m^{-3} consisted of 60% low volatility organic compounds (LVOCs), 30% semi-volatile (SVOCs), and 10% intermediate volatility (IVOCs) organic compounds (Fig. 3c). The estimated effective vaporization enthalpy was 100 ± 14 kJ mol^{-1} (Fig. 3a) and the effective accommodation coefficient was equal to 0.06 but with corresponding uncertainty range covering more than an order of magnitude (Fig. 3b). The corresponding TD thermogram and the dilution curve for Experiment 1 are depicted in Fig. 4. Almost all the COA evaporated at 200°C, while approximately 20% of the COA evaporated at ambient temperature after isothermal dilution. The model reproduced pretty well the measured MFR by the TD but tended to overpredict the measured evaporation during dilution. The model estimated that 25% of the COA evaporated at ambient temperature with the concentration decreasing to 19 µg m^{-3} instead of the observed 21 µg -m^{-3}. According to the model the small amount of IVOCs that existed initially in the particle phase evaporated at 50°C in the TD. The SVOCs evaporated at 125°C and the COA remaining at higher temperatures consisted entirely of LVOCs (Fig. 4). The IVOCs, according once more to the model, evaporated after 10 min of dilution and the SVOCs after approximately 30 min. The relatively prompt evaporation during dilution is interpreted by the model as evidence that any resistances to mass transfer in this system were modest. The fact that only 20% of the COA evaporated during these first few minutes, suggests that the contribution of the more volatile OA components (IVOCs and part of the SVOCs) were also modest. After this 20% of the evaporated the system reached equilibrium and evaporation stopped. Table S1 summarizes the estimated volatility distribution along with the estimated effective parameters that affect volatility and the calculated average volatilities for the two experiments.

Kostenidou et al. (2009) proposed the theta angle (θ) as an indicator of mass spectra similarity by treating AMS spectra as vectors and calculating the corresponding angle θ. Lower θ imply more similar spectra. Fig. 5a compares the average ~~initial~~ HR-ToF-AMS normalized mass spectra of the COA at ambient temperature (25°C) to the average normalized spectra in the TD at 200°C. The two spectra were calculated by averaging the corresponding measurements during the experiment. There was very little temporal variation of either the ambient temperature or thermodenuded spectra (theta angles less than 2 degrees). The 25°C and 200°C~~two~~ spectra were quite similar to each other having an angle θ of 11 degrees (R^2=0.958). This suggests that the least volatile COA components were quite similar to the total COA from the AMS' point of view. The AMS does examine mainly the small fragments of the corresponding compounds therefore the volatility differences in this case may be due mainly to the size of the molecules and not so much to their chemical characteristics (e.g., acids versus olefins). Fig. 5b depicts the comparison of HR-ToF-AMS mass spectra at the onset of dilution with that one hour later, and the one at the end of the experiment. The resulting θ angles between the compared mass spectra were 3 to 4 degrees (R^2 ranging from 0.994 to 0.997) showing the similarity of the average OA composition during the dilution experiment.

The estimated volatility distribution of Experiment 2 is shown in Fig. 2. The average $\log_{10}C^*$ was 0.05 μg m^{-3}. The COA consisted of 75% LVOCs and 25% of SVOCs (Fig. 3c). The vaporization enthalpy was 85 ± 9 kJ mol^{-1} (Fig. 3a) and the accommodation coefficient was equal to 0.07 (Fig. 3b). The ~~small~~ differences especially in the evaporation at the lower temperatures between the two experiments can be due to the differences in the COA produced in the two experiments. However, the θ angle for the two COA spectra in the two experiments was only 5°.

The thermogram of TD measurements and the corresponding dilution curve of Experiment 2 are depicted in Fig. 6. Almost all t~~T~~he COA evaporated ~~completely~~ at 225°C in the TD. 20% (from 7.5 to 6 μg m^{-3}) of the COA evaporated at ambient temperature during dilution. The model reproduced quite well the corresponding TD measurements below 75°C but tended to overpredict the observed evaporation at higher temperatures. At the same time the model tended to slightly underpredict the observed evaporation at room temperature.

According to the model the SVOCs evaporated at 130°C and the COA remaining at higher temperatures consisted entirely of LVOCs (Fig. 6c). During isothermal dilution the model predicted that after 10 minutes the SVOCs evaporated (Fig. 6d).

The TD measurements even at 250°C could be reproduced assuming that least volatile COA components had a $C^*=10^{-3}$ μg m^{-3}. However, the existence of components with even lower volatility (extremely low volatility organic compounds, ELVOCs) cannot be eliminated. Around 5% of the COA did not evaporate even at the highest temperature used in the system. Nie et al. (2017) have provided evidence about the connection of ambient ELVOCs with humic like substances (HULIS).

3.2 Sensitivity analysis

The sensitivity of the above results to the parameter estimation approach was investigated. Two types of sensitivity tests were conducted: one by assuming specific effective accommodation coefficients and estimating the volatility distributions and effective vaporization enthalpies and one by assuming different effective vaporization enthalpies and estimating the volatility distributions and accommodation coefficients using the approach of Karnezi et al. (2014).

3.2.1 Sensitivity to the accommodation coefficient

During these tests the volatility distributions and effective vaporization enthalpies were estimated for both experiments while assuming fixed accommodation coefficient values. Table S2 and Fig. S5 summarize the estimated volatility distributions during these tests. Assuming an accommodation coefficient of 0.01 which is approximately half an order of magnitude lower than the estimated one for the base case (0.01 instead of 0.06 for Experiment 1 and 0.07 for Experiment 2), the IVOC fraction remained the same but the SVOCs increased by 15% and the LVOCs decreased by the same amount compared to the base case results. Assuming an a_m equal to 0.1 the LVOCs increased by around 10% and the SVOCs decreased by the same amount, while the IVOCs remained once again the same (Fig. S5). For a further increase of a_m to unity the LVOCs increased by 15% and the SVOCs decreased by the same amount, while the IVOC fraction remained the same (Fig. S5). The estimated effective vaporization enthalpies were almost the same as those estimated in the base case (around 100 and 85 kJ mol^{-1} for Experiment 1 and Experiment 2 respectively) for all the investigated accommodation coefficients during this analysis (Table S2).

The predicted thermograms of the TD measurements and the corresponding predicted dilution curves of both experiments are shown in Fig. S6. For Experiment 1 assuming an accommodation coefficient equal to 0.01 the model performance deteriorated slightly at the low (25-80°C) and high (180-220°C) temperatures but improved in the middle (120-150°C). The cases of a_m=0.1 and 1.0 the predicted thermograms were almost the same with the one predicted in the base case (Fig S6a). The predicted dilution curve using an accommodation coefficient of 0.01 reproduced a little better the observed mass fraction values during the first hour of isothermal dilution compared to the base case. For an accommodation coefficient equal to unity the evaporation at ambient temperature was overestimated during the first hour of the experiment and for accommodation coefficient 0.1 the dilution curve was almost the same with that predicted for the base case (Fig. S6b). The predicted thermograms for Experiment 2 were quite similar for all accommodation coefficient examined (Fig. S6c). With the exception of the a_m=0.01 the other three simulations (for a_m= 0.07, 0.1 and 1.0) reproduced the dilution observations quite well (Fig. S6d).

Summarizing, varying the accommodation coefficient from 0.01 to 1.0 compared to the estimated 0.06-0.07 resulted in negligible changes in the estimated enthalpy of vaporization and the IVOC content of COA. The SVOCs and LVOCs changed by less than 15% in these tests. The deterioration in the performance of the model was small, underlying the difficulty of obtaining accurate values of the effective accommodation coefficient from such measurements in complex systems.

3.2.2 Sensitivity tests to vaporization enthalpies

During these tests the volatility distributions and effective accommodation coefficients were estimated for both experiments assuming values of the effective vaporization enthalpy. Values of 120 and 60 kJ mol^{-1} were used for both experiments to test the sensitivity of our results to ΔH_{vap}. These should be compared to the estimated values of 100 kJ mol^{-1} for the first experiment and 85 kJ mol^{-1} for the second.

For the high value of the vaporization enthalpy (120 kJ mol^{-1}) the estimated volatilities were lower by approximately half an order of magnitude compared to that of the base case (Table S2) for both experiments. The LVOCs increased by 5-10% and the SVOCs decreased by the same amount, while the IVOC fraction remained approximately the same. Fig. S7 shows the estimated volatility distributions and COA compositions of both experiments for all the cases of this analysis. The estimated accommodation coefficients were almost half an order of magnitude lower compared to that of the base case values (Table S2).

Assuming a vaporization enthalpy of 60 kJ mol^{-1} the corresponding volatilities for both experiments increased by approximately a factor of 2. The LVOC fraction for this case decreased by 5-10% and a corresponding increase was estimated for the SVOCs. Once again the IVOC fraction remained the same. The estimated accommodation coefficients were similar to the base case.

For both experiments the increase of the vaporization enthalpy resulted in an overprediction of the evaporation in the TD failing to reproduce the results of Experiment 1. On the other hand the corresponding decrease in vaporization enthalpy led to the opposite problem. The changes in the model's ability to reproduce the dilution measurements were, as expected, less sensitive to ΔH_{vap}.

The above results suggest that changes in vaporization enthalpy by 15-40 kJ mol^{-1} produce changes in the volatility distribution by less than half an order of magnitude. Higher values of the enthalpy are balanced with lower volatilities and vice versa. The accommodation coefficient is more sensitive in this case to higher vaporization enthalpy values than to lower ones.

4. Benefits of combining TD and i~~I~~sothermal dilution

In order to evaluate the benefits of the combination of thermodenuder and isothermal dilution measurements the above results were compared to the results obtained by using only the thermodenuder data. The algorithm of Karnezi et al. (2014) was used once more to estimate the volatility distributions, the vaporization enthalpy, and accommodation coefficient based only on the thermodenuder measurements.

The corresponding results are shown in Fig. 7 and Table S1. The combination of thermodenuder and dilution measurements resulted in a less volatile COA in both cases. In Experiment 1 the average volatility was reduced by almost half an order of magnitude (from 0.44 to 0.1 μg m^{-3}) due to the inclusion of dilution data. For Experiment 2 the corresponding reduction was approximately a factor of 2. The combined approach suggests that COA consisted of 60% LVOCs, 30% SVOCs, and 10% IVOCs while the TD-only approach results in almost 40% LVOCs, 50% SVOCs, and 10% IVOCs for Experiment 1. For Experiment 2 the combined approach once again suggested that the COA consisted of 77% LVOCs and 23% SVOCs, while the TD-only approach suggested of 68% LVOCs and 32% SVOCs.

In both experiments the use of only the thermodenuder measurements resulted in an overestimation of the SVOCs by 10-20% and a subsequent reduction by the same amount of the LVOCs. The combination of thermodenuder and isothermal dilution measurements led to a reduction of the uncertainty range for the more volatile OA components with effective saturation concentrations from 10 to 1000 μg m^{-3}. The uncertainty ranges of the estimated effective vaporization enthalpies were reduced from 15-20 kJ mol^{-1} to 10-15 kJ mol^{-1} when the dilution data were included in the analysis. There was little change in the uncertainty of the accommodation coefficients.

5. Conclusions

The approach of Grieshop et al. (2009) ~~A new experimental method was developed~~ for the determination of the organic aerosol (OA) volatility distribution combining thermodenuder and isothermal dilution measurements is extended and combined with the optimization algorithm ~~along with the approach~~ proposed by Karnezi et al. (2014). The combination of TD and isothermal dilution for the estimation of the volatility distribution was tested for cooking OA from meat grilling. Size dependent losses were taken into account for the correction of both thermodenuder and dilution measurements.

All the COA evaporated in the TD at 225°C while 80% remained after dilution by a factor of 10 at ambient temperature. The COA average volatility was between 0.05 and 0.1 μg m^{-3}. The COA at around 500 μg m^{-3} consisted of 60-75% LVOCs, 25-30% SVOCs, and a small fraction (10%) of IVOCs. The estimated effective vaporization enthalpy was 100 ± 15 kJ mol^{-1}, and the effective accommodation coefficient was 0.06-0.07 with corresponding uncertainty range of one order of magnitude. These values should be applicable to COA produced during pork meat charbroiling.

Changes of the accommodation coefficient of half an order of magnitude result in similar magnitude changes of the average volatility. The estimated vaporization enthalpy was almost the same with the reported value of the base case. Similar results were found for a change of the effective vaporization enthalpy by 15-40 kJ mol^{-1}. The COA composition exhibited changes in the LVOC and SVOC fractions by 5-15% while the IVOCs remained practically the same.

The use of only TD measurements resulted in an overestimation of the SVOC fraction of COA leading to a shifting of volatility towards higher values. Combination of TD and dilution results in a lower uncertainty of the estimated effective vaporization enthalpy. The dilution measurements also help constrain the contribution of the more volatile OA components (SVOCs) to the total OA concentration. On the other hand, the volatility distribution of the LVOCs is based mainly on the TD data.~~as well as the SVOC content of the OA.~~

Acknowledgements

This research was supported by the US National Science Foundation (Award number 1455244) and the Greek "ARISTEIA" action of the “Operational Programme Education and Lifelong Learning” co-funded by the European Social Fund (ESF) and National Resources.

References

An, W. J., Pathak, R. K., Lee, B. H. and Pandis, S. N.: Aerosol volatility measurement using an improved thermodenuder: Application to secondary organic aerosol, J. Aerosol Sci., 38, 305–314, 2007.

~~Barmet, P., Dommen, J., DeCarlo, P. F., Tritscher, T., Praplan, A. P., Platt, S. M., Prévôt, A. S. H., Donahue, N. M. and Baltensperger, U.: OH clock determination by proton transfer reaction mass spectrometry at an environmental chamber, Atmos. Meas. Tech., 5, 647–656, 2012.~~

Burtscher, H., Baltensperger, U., Bukowiecki, N., Cohn, P., Hüglin, C., Mohr, M., Matter, U., Nyeki, S., Schmatloch, V., Streit, N. and Weingartner, E.: Separation of volatile and non-volatile aerosol fractions by thermodesorption: Instrumental development and applications, J. Aerosol Sci., 32, 427–442, 2001.

Caiazzo, F., Ashok, A., Waitz, I. A., Yim, S. H. L. and Barrett, S. R. H.: Air pollution and early deaths in the United States. Part I: Quantifying the impact of major sectors in 2005, Atmos. Environ., 79, 198–208, 2013.

Canagaratna, M. R., Jayne, J. T., Jimenez, J. L., Allan, J. D., Alfarra, M. R., Zhang, Q., Onasch, T. B., Drewnick, F., Coe, H., Middlebrook, A. M., Delia, A. E., Williams, L.

R., Trimborn, A. M., Northway, M. J., DeCarlo, P. F., Kolb, C. E., Davidovits, D. R.: Chemical and microphysical characterization of ambient aerosols with the Aerodyne Aerosol mass Spectrometer, Mass Spectrom. Rev., 26, 185–222, 2007.

Cappa, C. D.: A model of aerosol evaporation kinetics in a thermodenuder, Atmos. Meas. Tech., 3, 579–592, 2010.

Cappa, C. D. and Jimenez, J. L.: Quantitative estimates of the volatility of ambient organic aerosol, Atmos. Chem. Phys., 10, 5409–5424, 2010.

Cappa, C. D. and Wilson, K. R.: Evolution of organic aerosol mass spectra upon heating: Implications for OA phase and partitioning behavior, Atmos. Chem. Phys., 11, 1895–1911, 2011.

Decarlo, P. F., Kimmel, J. R., Trimborn, A., Northway, M. J., Jayne, J. T., Aiken, A. C., Gonin, M., Fuhrer, K., Horvath, T., Docherty, K. S., Worsnop, D. R. and Jimenez, J. L.: Aerosol Mass Spectrometer, Anal. Chem., 78, 8281–8289, 2006.

Donahue, N. M., Robinson, A. L., Stanier, C. O. and Pandis, S. N.: Coupled partitioning, dilution, and chemical aging of semivolatile organics, Environ. Sci. Technol., 40, 2635–2643, 2006.

Donahue, N. M., Kroll, J. H., Pandis, S. N. and Robinson, A. L.: A two-dimensional volatility basis set-Part 2: Diagnostics of organic-aerosol evolution, Atmos. Chem. Phys., 12, 615–634, 2012.

IPCC (Intergovernmental Panel on Climate Change): Climate Change 2014: Mitigation of Climate Change. Contribution of Working Group III to the Fifth Assessment Report of the Intergovernmental Panel on Climate Change, Cambridge University Press, Cambridge, UK and New York, 2014.

Faulhaber, A. E., Thomas, B. M., Jimenez, J. L., Jayne, J. T., Worsnop, D. R. and Ziemann, P. J.: Characterization of a thermodenuder-particle beam mass spectrometer system for the study of organic aerosol volatility and composition, Atmos. Meas. Tech., 2, 15–31, 2009.

Grieshop, A. P., Miracolo, M. A., Donahue, N. M. and Robinson, A. L.: Constraining the volatility distribution and gas-particle partitioning of combustion aerosols using isothermal dilution and thermodenuder measurements, Environ. Sci. Technol., 43, 4750–4756, 2009.

Huffman, J. A., Docherty, K. S., Aiken, A. C., Cubison, M. J., Ulbrich, I. M., DeCarlo, P. F., Sueper, D., Jayne, J. T., Worsnop, D. R., Ziemann, P. J. and Jimenez, J. L.: Chemically-resolved aerosol volatility measurements from two megacity field studies, Atmos. Chem. Phys., 9, 7161-7182, 2009.

Kalberer, M., Paulsen, D., Sax, M., Steinbacher, M., Dommen, J., Prévôt, A. S. H., Fisseha, R., Weingartner, E., Frankevich, V., Zenobi, R. and Baltensperger, U.: Identification of polymers as major components of atmospheric organic aerosol, Science, 303, 1659–1662, 2004.

Kaltsonoudis, C., Kostenidou, E., Louvaris, E. Psichoudaki, M., Tsiligiannis, E., Florou, K., Liangou, A., and Pandis, S. N.: Characterization of fresh and aged organic aerosol emissions from meat charbroiling, Atmos. Chem. Phys. Discuss., doi:10.5194/acp-2016-979, 2016a.

Kaltsonoudis, C., Kostenidou, E., Florou, K., Psichoudaki, M., and Pandis, S. N.: Temporal variability and sources of VOCs in urban areas of the eastern Mediterranean, Atmos. Chem. Phys., 16, 14825–14842, 2016b.

Karnezi, E., Riipinen, I. and Pandis, S. N.: Measuring the atmospheric organic aerosol volatility distribution: A theoretical analysis, Atmos. Meas. Tech., 7, 2953–2965, 2014.

Kolesar, K. R., Chen, C., Johnson, D. and Cappa, C. D.: The influences of mass loading and rapid dilution of secondary organic aerosol on particle volatility, Atmos. Chem. Phys., 15, 9327–9343, 2015.

Kostenidou, E., Lee, B. H., Engelhart, G. J., Pierce, J. R. and Pandis, S. N.: Mass spectra deconvolution of low, medium, and high volatility biogenic secondary organic aerosol, Environ. Sci. Technol., 43, 4884–4889, 2009.

Lee, B. H., Kostenidou, E., Hildebrandt, L., Riipinen, I., Engelhart, G. J., Mohr, C., Decarlo, P. F., Mihalopoulos, N., Prévôt, A. S. H., Baltensperger, U. and Pandis, S. N.: Measurement of the ambient organic aerosol volatility distribution: Application during the Finokalia Aerosol Measurement Experiment (FAME-2008), Atmos. Chem. Phys., 10, 12149–12160, 2010.

Lee, B. H., Pierce, J. R., Engelhart, G. J. and Pandis, S. N.: Volatility of secondary organic aerosol from the ozonolysis of monoterpenes, Atmos. Environ., 45, 2443–2452, 2011.

Louvaris, E. E., Florou, K., Karnezi, E., Papanastasiou, D. K., Gkatzelis, G. I., and Pandis, S. N.: Volatility of source apportioned wintertime organic aerosol in the city of Athens, Atmos. Environ., doi.org/10.1016/j.atmosenv.2017.03.042, 2017.

Nie, W., Hong, J., Hame, S. A. K., Ding, A., Li, Y., Yan, C., Hao, L., Mikkila, J., Zheng, L., Xie, Y., Zhu, C., Xu, Z., Chi, X., Huang, X., Zhou, Y., Lin, P., Virtanen, A., Worsnop, D. R., Kulmala, M., Ehn, M., Yu, J., Kerminen, V. M., and Tuukka, P.: Volatility of mixed atmospheric humic-like substances and ammonium sulfate particles, Atmos. Chem. Phys., 17, 3659-3672, 2017.

Pathak, R. K., Presto, A. A., Lane, T. E., Stanier, C. O., Donahue, N. M. and Pandis, S. N.: Ozonolysis of α-pinene: parameterization of secondary organic aerosol mass fraction, Atmos. Chem. Phys., 7, 3811–3821, 2007.

Pope, C. A., Ezzati, M., Dockery, D. W.: Fine-particulate air pollution and life expectancy in the United States, N. Engl. J. Med., 360, 376–386, 2009.

Riipinen, I., Pierce, J. R., Donahue, N. M. and Pandis, S. N.: Equilibration time scales of organic aerosol inside thermodenuders: Evaporation kinetics versus thermodynamics, Atmos. Environ., 44, 597–607, 2010.

Saleh, R., Walker, J. and Khlystov, A.: Determination of saturation pressure and enthalpy of vaporization of semi-volatile aerosols: The integrated volume method, J. Aerosol Sci., 39, 876–887, 2008.

Saleh, R., Khlystov, A. and Shihadeh, A.: Determination of evaporation coefficients of ambient and laboratory-generated semivolatile organic aerosols from phase equilibration kinetics in a thermodenuder, Aerosol Sci. Technol., 46, 22–30, 2012.

Saleh, R., Donahue, N. M. and Robinson, A. L.: Time scales for gas-particle partitioning equilibration of secondary organic aerosol formed from alpha-pinene ozonolysis, Environ. Sci. Technol., 47, 5588–5594, 2013.

Wehner, B., Philippin, S. and Wiedensohler, A.: Design and calibration of a thermodenuder with an improved heating unit to measure the size-dependent volatile fraction of aerosol particles, J. Aerosol Sci., 33, 1087–1093, 2002.

Wehner, B., Philippin, S., Wiedensohler, A., Scheer, V. and Vogt, R.: Variability of non-volatile fractions of atmospheric aerosol particles with traffic influence, Atmos. Environ., 38, 6081–6090, 2004.

Zhang, Q., Jimenez, J. L., Canagaratna, M. R., Allan, J. D., Coe, H., Ulbrich, I., Alfarra, M. R., Takami, A., Middlebrook, A. M., Sun, Y. L., Dzepina, K., Dunlea, E., Docherty, K., DeCarlo, P. F., Salcedo, D., Onasch, T., Jayne, J. T., Miyoshi, T., Shimono, A., Hatakeyama, S., Takegawa, N., Kondo, Y., Schneider, J., Drewnick, F., Borrmann, S., Weimer, S., Demerjian, K., Williams, P., Bower, K., Bahreini, R., Cottrell, L., Griffin, R. J., Rautiainen, J., Sun, J. Y., Zhang, Y. M. and Worsnop, D. R.: Ubiquity and dominance of oxygenated species in organic aerosols in anthropogenically-influenced Northern Hemisphere midlatitudes, Geophys. Res. Lett., 34, doi:10.1029/2007GL029979, 2007.

Table 1: Summary of the experimental conditions

Experiment	Initial concentration ($\mu g\ m^{-3}$)		Initial volume mode diameter (nm)		Average dilution ratio
	Main chamber	Dilution chamber	Main chamber	Dilution chamber	Dilution chamber
1	541	26.5	248	210	11 ± 0.5
2	632	7.4	284	218	14 ± 0.5

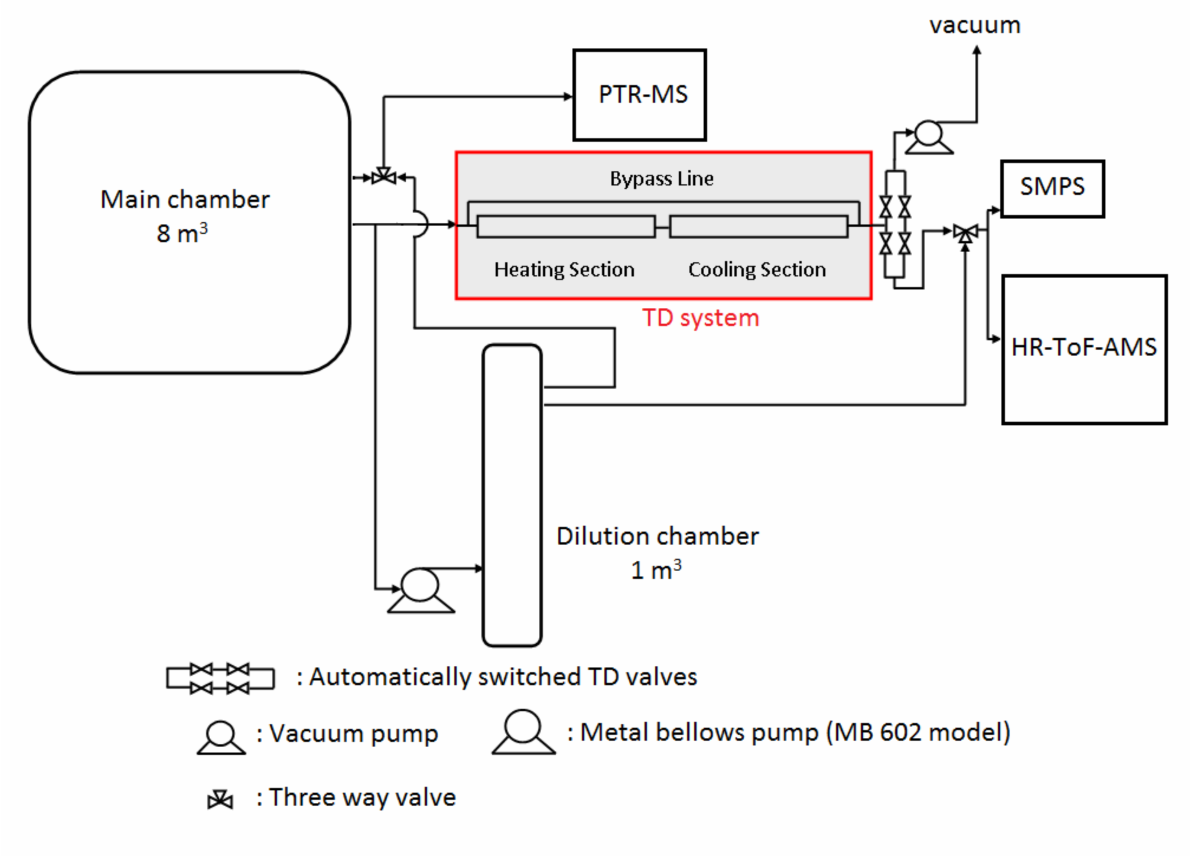

Figure 1: Schematic of the experimental setup used in the experiments. The COA in the main chamber was characterized using a TD a HR-ToF-AMS, and an SMPS. A metal bellows pump was used to transfer OA from the main to the dilution chamber. The COA in the dilution chamber was measured by the HR-ToF-AMS and the SMPS. A PTR-MS was used to measure the dilution ratio.

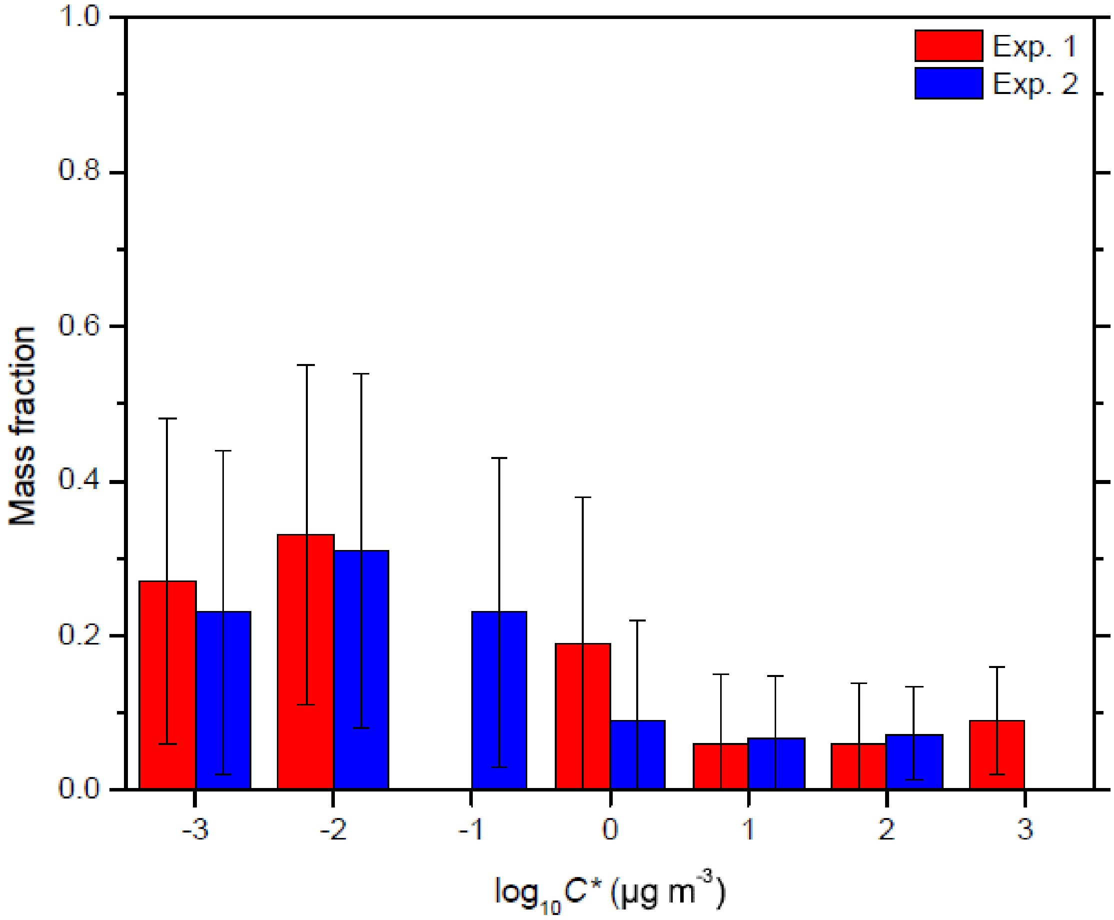

Figure 2: Estimated volatility distributions for Experiment 1 (red bars) and for Experiment 2 (blue bars) using the approach of Karnezi et al. (2014). The error bars represent the uncertainty of the estimated mass fractions.

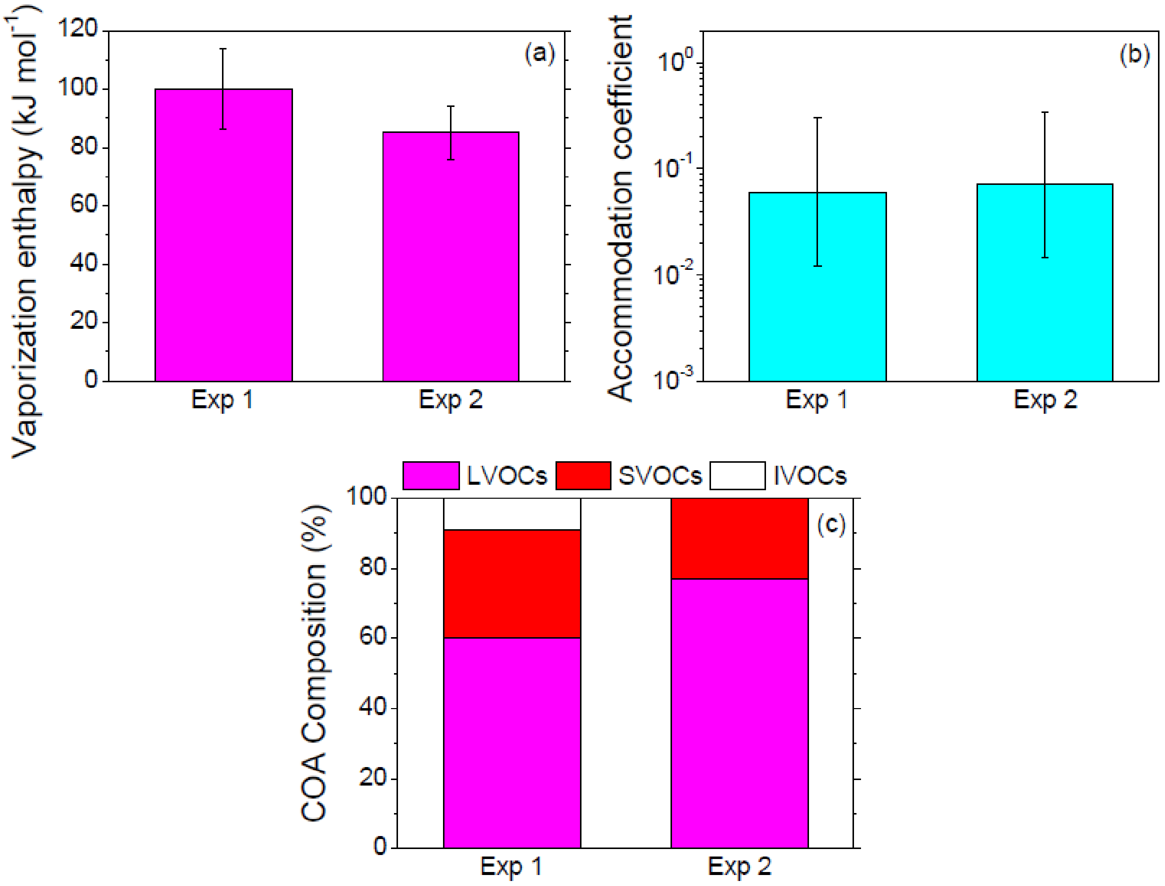

Figure 3: (a) Estimated effective vaporization enthalpies along with their uncertainties for both experiments using the approach of Karnezi et al. (2014). (b) Estimated effective accommodation coefficients along with their uncertainties for both experiments. (c) COA mass composition of both experiments. LVOCs are represented in magenta, SVOCs in red, and IVOCs in white.

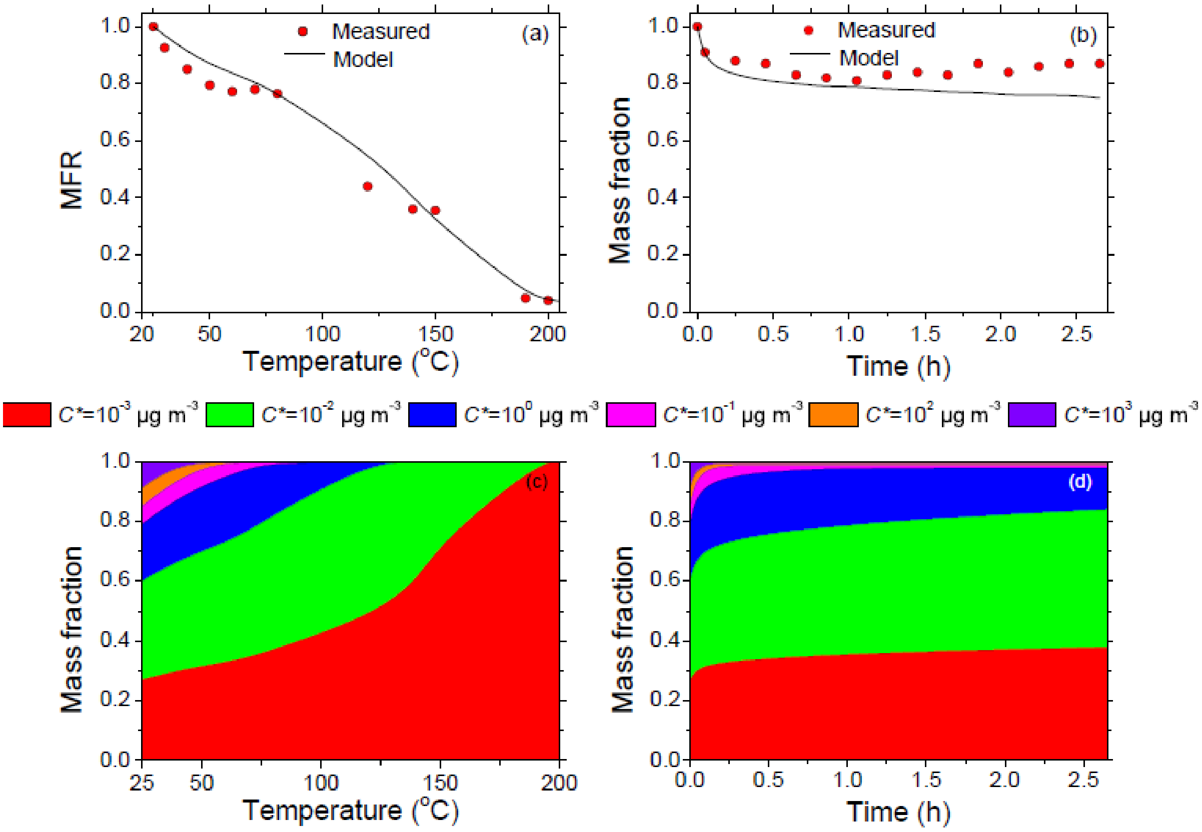

Figure 4: (a) Thermogram of the OA TD measurements of Experiment 1. Red circles represent the loss corrected measurements and the black line represents the best fit estimated by the model of Karnezi et al. (2014) (b) Mass fraction during isothermal dilution as a function of time of Experiment 1. Red circles represent the loss corrected measurements and the black line the estimated best model fit. (c) COA mass fraction for different effective saturation concentrations as a function of TD temperature. Red color represents the contribution of the effective saturation concentration $C^* = 10^{-3}$ µg m^{-3}, green the contribution of the $C^* = 10^{-2}$ µg m^{-3}, blue the $C^* = 1$ µg m^{-3}, magenta the $C^* = 10$ µg m^{-3}, orange the $C^* = 10^{2}$ µg m^{-3}, and violet the $C^* = 10^{3}$ µg m^{-3}. (d) COA mass fraction for different effective saturation concentrations as a function of time during isothermal dilution.

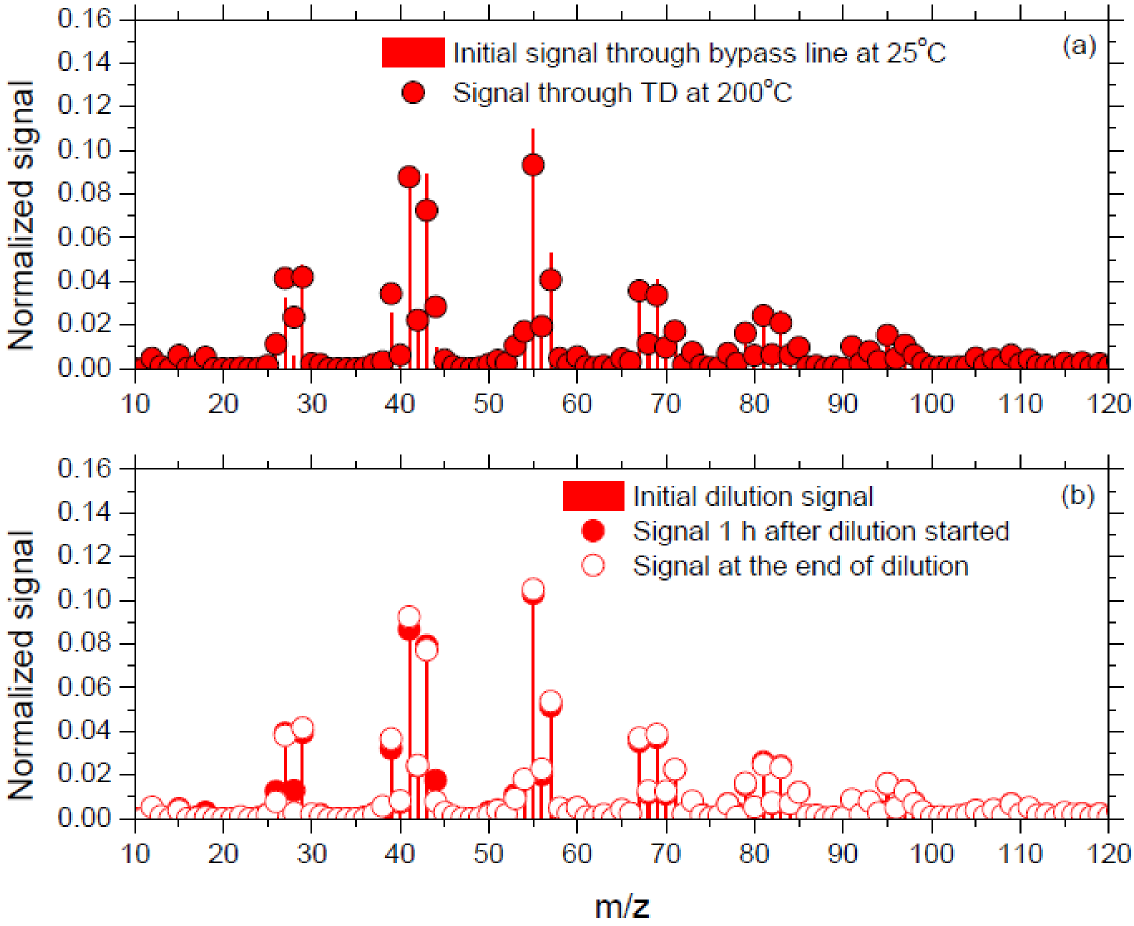

Figure 5: (a) Normalized HR-ToF-AMS mass spectra of the initial measurements at ambient temperature through the bypass line (red bars) compared to those measured in the TD at 200°C (red circles). (b) Normalized HR-ToF-AMS mass spectra at the onset of dilution experiment (red bars) compared to those measured after one hour (solid circles), and to those measured at the end of the experiment (open circles).

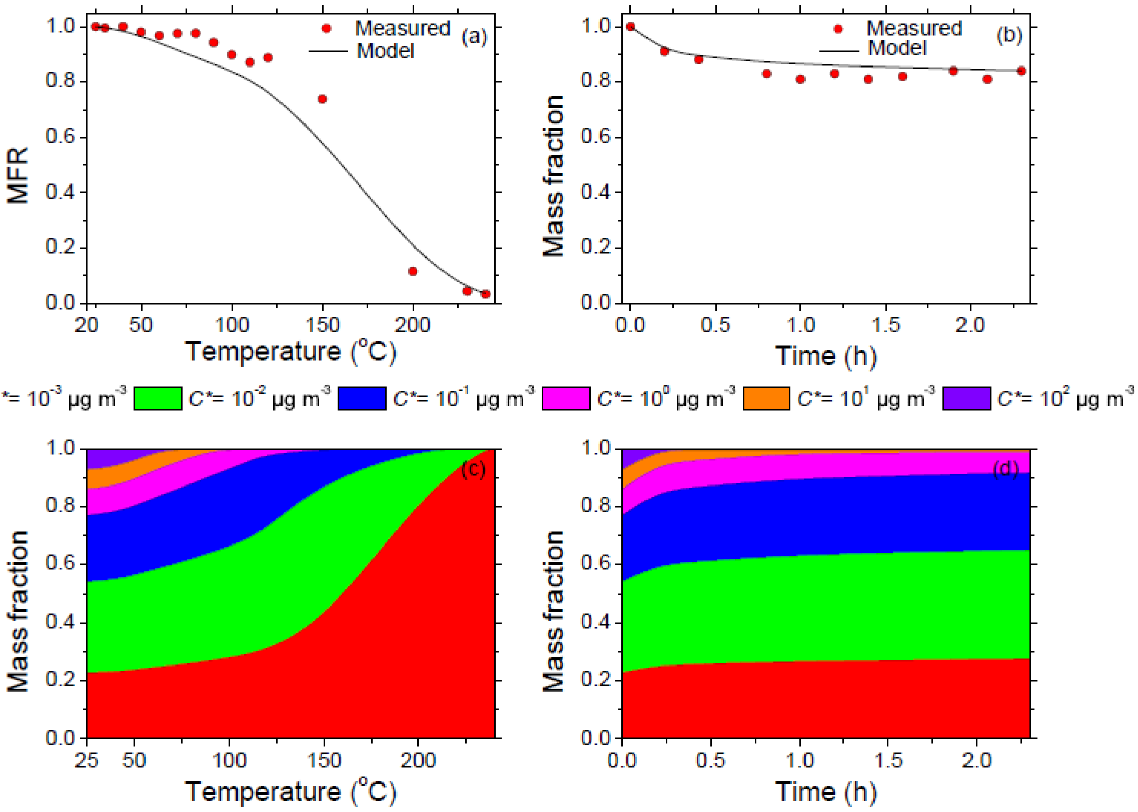

Figure 6: (a) Thermogram of the OA TD measurements of Experiment 2. Red circles represent the loss corrected measurements and the black line represents the best fit estimated by the model of Karnezi et al. (2014). (b) Mass fraction during isothermal dilution as a function of time of Experiment 2. Red circles represent the loss corrected measurements and the black line the estimated best model fit. (c) COA mass fraction for different effective saturation concentrations as a function of TD temperature. Red color represents the contribution of the effective saturation concentration $C^* = 10^{-3}$ μg m^{-3}, green the contribution of the $C^* = 10^{-2}$ μg m^{-3}, blue the $C^* = 10^{-1}$ μg m^{-3}, magenta the $C^* = 1$ μg m^{-3}, orange the $C^* = 10$ μg m^{-3}, and violet the $C^* = 10^2$ μg m^{-3}. (d) COA mass fraction for different effective saturation concentrations as a function of time during isothermal dilution.

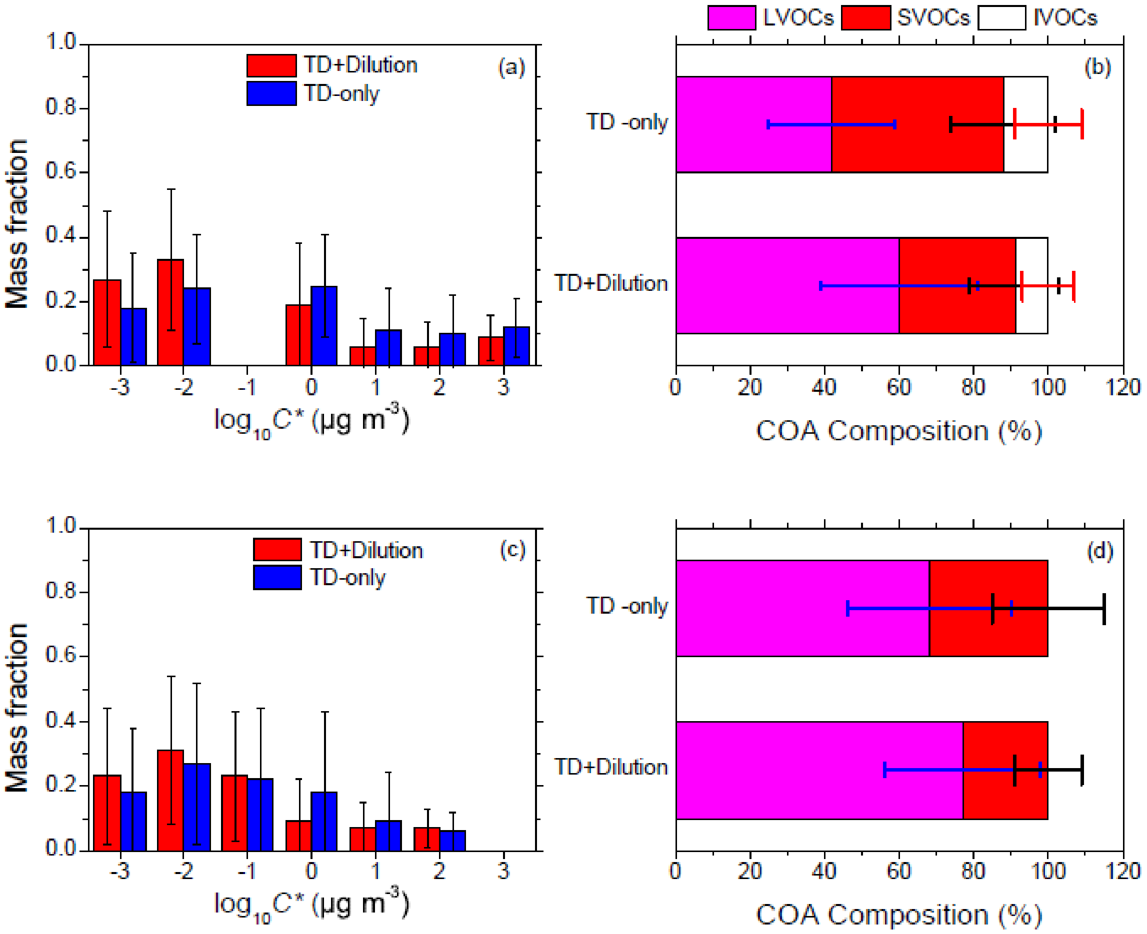

Figure 7: (a) Estimated volatility distributions of the COA along with their uncertainties of Experiment 1 using the approach of Karnezi et al. (2014). Red bars represent the volatility distribution using the combination of thermodenuder and isothermal dilution measurements whereas blue bars represent the volatility distribution using only thermodenuder measurements (b) Corresponding COA compositions for the two cases of (a) along with their corresponding uncertainties (±1 standard deviation). LVOCs are in magenta, SVOCs in red, and IVOCSs in white. The uncertainty range of IVOCs, SVOCs and LVOCs are shown in red, black and blue respectively. (c) Estimated volatility distributions of the COA of Experiment 2 using the approach of Karnezi et al. (2014). Red bars represent the volatility distribution using the combination of thermodenuder and isothermal dilution measurements whereas blue bars represent the volatility distribution using only thermodenuder measurements. (d) Corresponding COA compositions for the two cases of (c) along with their corresponding uncertainties (±1 standard deviation). LVOCs are in magenta and SVOCs in red. The uncertainty ranges of SVOCs and LVOCs are shown in black, and blue respectively.